Highlights

- Dietary theobromine (TB) induces browning of subcutaneous white adipose tissue (WAT).
- TB induces thermogenic and mitochondrial proteins in subcutaneous WAT.
- TB changes gene expression profile for browning of subcutaneous WAT.
- PPARγ activation is required for TB-induced browning in mice primary adipocytes.
- TB increases mitochondria mass through inhibition of mitophagy.

Graphic abstract

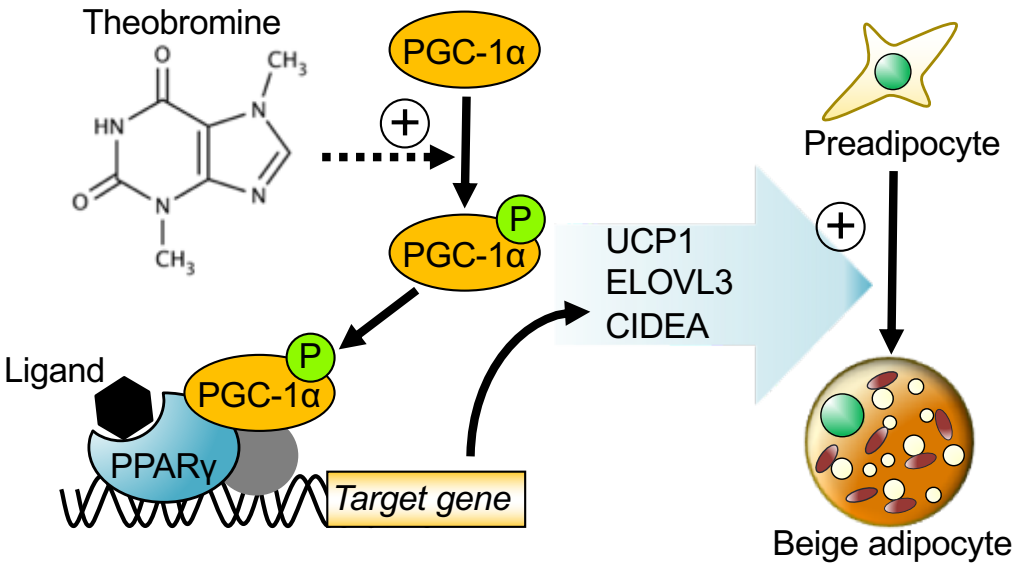

Theobromine enhances the conversion of white adipocytes into beige adipocytes in a PPARγ activation-dependent manner

Emi Tanaka[a], Takakazu Mitani[a, b*], Momona Nakashima[a], Eito Yonemoto[b], Hiroshi Fujii[b], and Hitoshi Ashida[c]

[a]Division of Food Science and Biotechnology, Graduated School of Science and Technology, Shinshu University, 8304 Minami-minowa, Kamiina, Nagano, 3994598, Japan.

[b]Department of Agricultural and Life Sciences, Faculty of Agriculture, Shinshu University, 8304 Minami-minowa, Kamiina, Nagano, 3994598, Japan.

[c]Department of Agrobioscience, Graduate School of Agricultural Science, Kobe University, 1-1 Rokkodai-cho, Nada-ku, Kobe, Hyogo, 6578501, Japan.

Running title: Theobromine promotes the browning of white adipocytes

*; To whom correspondence should be addressed: Takakazu Mitani, Ph.D., Department of Agricultural and Life Sciences, Faculty of Agriculture, Shinshu University, 8304 Minami-minowa, Kamiina, Nagano, Japan. Tel.: +81-265-77-1608, Fax: +81-265-77-1315; E-mail: mitani@shinshu-u.ac.jp

Abbreviations: adenosine receptor, AR; β3-adrenergic receptor, β3-AR; brown adipose tissue, BAT; Dulbecco's modified Eagle medium, DMEM; Fetal bovine serum, FBS; Non-esterified fatty acid, NEFA; Oxygen consumption rate, OCR; peroxisome

24 proliferator-activated receptor γ coactivator-1α, PGC-1α; peroxisome proliferator-
25 activated receptor, PPAR; PR domain containing 16, PRDM16; quantitative real-time
26 PCR, qPCR; relative light units, RLU; theobromine, TB; uncoupling protein 1, UCP1;
27 white adipose tissue, WAT
28

Abstract

The adipocytes play an important role in driving the obese-state—white adipose tissue (WAT) stores the excess energy as fat, wherein brown adipose tissue (BAT) is responsible for energy expenditure via the thermoregulatory function of uncoupling protein 1 (UCP1)—the imbalance between these two onsets obesity. Moreover, the anti-obesity effects of brown-like-adipocytes (beige) in WAT are well documented. Browning, the process of transformation of energy-storing into energy-dissipating adipocytes, is a potential preventive strategy against obesity and its related diseases. In the present study, to explore an alternative source of natural products in the regulation of adipocyte transformation, we assessed the potential of theobromine (TB), a bitter alkaloid of the cacao plant, inducing browning in mice (*in vivo*) and primary adipocytes (*in vitro*). Dietary supplementation of TB significantly increased skin temperature of the inguinal region in mice and induced the expression of UCP1 protein. It also increased the expression levels of mitochondrial marker proteins in subcutaneous adipose tissues but not in visceral adipose tissues. The microarray analysis showed that TB supplementation upregulated multiple thermogenic and beige adipocyte marker genes in subcutaneous adipose tissue. Furthermore, in mouse-derived primary adipocytes, TB upregulated the expression of the UCP1 protein and mitochondrial mass in a PPARγ ligand-dependent manner. It also increased the phosphorylation levels of PPARγ coactivator 1α without affecting its protein expression. These results indicate that dietary supplementation of TB induces browning in subcutaneous WAT and enhances PPARγ-induced UCP1 expression *in vitro*, suggesting its potential to treat obesity.

Keywords: Autophagy; Browning; Beige adipocyte, Theobromine; Peroxisome proliferator-activated receptor γ

1. Introduction

Obesity, caused by excessive accumulation of fat in the body without being consumed, is a serious health problem worldwide. It is associated with the incidence of several obesity-related diseases, including type 2 diabetes mellitus, cardiovascular disease and hypertension [1]. Mammals have two different types of adipose tissues: white adipose tissues (WAT) and brown adipose tissues (BAT). WAT stores energy in the form of triglycerides, and WAT hypertrophy by excessive lipid accumulation leads to obesity. In contrast, BAT accelerates the metabolism of triglycerides through β-oxidation and releases energy in the form of heat by uncoupling the respiratory chain through the uncoupling protein 1 (UCP1) [2]. Moreover, an inverse correlation between the amounts of BAT and brown adipocytes with high body mass index, hyperglycemia, and adiposity has also been reported [3]. Therefore, the therapeutic strategies to alleviate obesity target the enhancement of BAT formation and activation of brown adipocytes. However, brown adipocytes that are abundant in newborns decrease significantly in adults with growth. In contrast, brown-like adipocytes, also known as beige or brite (brown-in-white) adipocytes, are newly reported as adipocytes located in the WAT in adult humans and have a similar biochemical and morphological phenotype as brown adipocytes [4]. Similar to brown adipocytes, beige adipocytes are defined by high mitochondria content, multilocular lipid droplet morphology, and the expression of a core set of brown adipocyte-specific genes, such as *Ucp1*, *Cidea*, and *Elvol3* [5]. In mice, the conversion of white adipocytes into

beige adipocytes, known as "browning," has been reported to be induced by cold exposure via the activation of proliferator-activated receptor γ (PPARγ) and β-adrenergic stimulation [6]. Moreover, it has been reported that the subcutaneous adipocytes have a greater differentiation potential compared to visceral adipocytes suggesting that the subcutaneous adipocytes are more likely to induce browning than visceral adipocytes [5]. Recent studies indicated the existence of beige adipocytes in adult humans [7]; therefore, it is expected that promoting the browning of white adipocytes could be a beneficial health strategy against obesity and its related diseases.

The PPARs are a group of nuclear receptor proteins that function as transcription factors regulating the expression of genes involved in metabolism and cellular differentiation [8]. Of them, PPARγ is the master regulator or crucial determinant of adipocyte differentiation. It not only regulates the differentiation of white adipocytes but is also involved in the browning of white adipocytes [8]. In rodent models, it has been shown that the synthetic ligand-bound PPARγ directly binds to PPAR-response elements (PPREs) on the enhancer region of brown-adipocyte-selective and thermogenic genes, including *Ucp1*, resulting in browning of white adipocyte [8–10]. The other major regulators of browning are the PR domain containing 16 (PRDM16) and PPARγ coactivator 1α (PGC-1α). Knockdown of PRDM16 expression decreases thermogenic gene expression and browning in subcutaneous adipocytes, whereas PPARγ agonist increases UCP1 expression through stabilization of PRDM16 protein in WAT [11,12]. Nuclear PGC-1α enhances the expression of thermogenic genes through interaction with PPARγ. Additionally, it has been shown that the function of PGC-1α is regulated by its expression levels and phosphorylation status. In brown adipocytes, the phosphorylation

of PGC-1α by p38 mitogen-activated protein kinase is necessary for driving *UCP1* gene transcription [13]. Moreover, it is known that PPARγ regulates not only browning but also white adipocyte differentiation; hence, activation of PPARγ by excessive synthetic ligands might cause side effects, such as weight gain [14]. Therefore, it is important to identify effective alternative compounds that could induce browning from safe food-derived compounds.

Cacao, a widely consumed fruit, is rich in many polyphenols, including catechins and procyanidins; therefore, it has gained increasing research interest. However, the health benefits of theobromine (TB), a methylxanthine found in cacao beans (~ 1%) [15], have not been explored fully [16–18]. Our previous study showed that short-term administration of methylxanthine derivative-rich cacao extract suppresses weight gain in mice [19]. In addition, TB suppresses adipocyte differentiation and adipogenesis *in vitro* and *in vivo* [20]. These studies, though demonstrated the efficacy of TB to suppress obesity, the effect of TB intake on the browning of WAT has not been explored. Therefore, the present study investigates the effects of TB intake on the regulation of browning. It demonstrates an increase in UCP1 protein levels and mitochondria mass in subcutaneous WAT, increasing heat production and browning of subcutaneous WAT. Furthermore, we suggest that the activation of PPARγ is required for TB-induced adipocyte browning in mice primary adipocytes.

2. Experimental Section

2.1. Animal experiments

Six-week-old male C57BL/6N mice were purchased from Japan SLC, Inc. (Shizuoka, Japan) and housed under controlled temperature (20 ± 3°C) with a 12 h light/dark cycle (lights were turned on at 8:00 am). The mice had free access to food and water and were acclimated for 7 days before the experiments. The mice were randomly divided into three groups and fed AIN-93 M diet containing different concentrations of TB —0% (CTL group), 0.05% (0.05% TB group), and 0.1% (0.1% TB group)—for 63 days (n = 6). At the end of the experiment, the skin temperature of mice was measured using a thermographic camera (FLIR Systems), and then the mice were sacrificed under anesthesia. Adipose tissues and plasma samples and tissues were collected under anesthesia, and the samples were stored frozen (−80℃) until analysis. Plasma unesterified fatty acid (NEFA) was determined by NEFA C-Test Wako (Fujifilm Wako Pure Chemical Industries, Osaka, Tokyo). All animal experiments conformed to the protocols approved by the Institutional Animal Care and Use Committee of Shinshu University Animal Experimentation Regulations (Permission Number 290075 and 019024) and the Guide for Care and Use of Laboratory Animals (NIH Publications No. 8023, revised 1978).

2.2. Cell culture

Adipose stromal cells (ASCs) were isolated and cultured following a previously described method [21] with minor modifications. Briefly, ASCs were isolated from inguinal WAT of mice. After digestion with collagenase II and centrifugation, preadipocytes were cultured in Dulbecco's modified Eagle's medium (DMEM)

144 supplemented with 20% fetal bovine serum (FBS), 100 μg/mL streptomycin, and 100
145 units/mL penicillin. After reaching confluency, the cells were treated with a
146 differentiation-inducing cocktail (DIC; 1 μM dexamethasone, 0.5 mM 3-isobutyl-1-
147 methylxanthine, 10 μg/mL insulin, 8 μg/mL biotin, and 10 μM rosiglitazone) in DMEM
148 with high glucose (4.5 g/L glucose), supplemented with 10% FBS for the first 2 days.
149 Then the cells were cultured in the same medium with or without TB in the presence of
150 insulin (10 μg/mL) and biotin (8 μg/mL) for another 5 days (total 7 days). The medium
151 was exchanged every 2 days. The mouse 3T3-L1 adipocytes were cultured following the
152 method described previously [20].
153
154 *2.3. Microarray analysis*
155
156 DNA microarray analyses were carried out by a Kurabo custom analysis service
157 (Kurabo Industries Ltd., Osaka, Japan). In brief, total RNA (100 ng) was prepared from
158 inguinal WAT in the control group and 0.1% TB group ($n = 2$) using the GeneChip WT
159 PLUS Reagent Kit (Thermo Scientific) according to the manufacturer's instructions. The
160 resultant single-strand cDNA was fragmented and labeled with biotin, then hybridized to
161 the Gene Chip Clariom S Mouse Assay (Thermo Scientific). The arrays were washed,
162 stained, and scanned using the Affymetrix 450 Fluidics Station and GeneChip Scanner
163 3000 7G (Thermo Scientific) according to the manufacturer's recommendations.
164 Expression values were generated using Expression Console software, version 1.3
165 (Thermo Scientific), with default robust multichip analysis parameters. The fold changes
166 in expression between control and 0.1% TB groups were calculated, log 2-transformed,

and further classified as not changed, increased (signal log ratio change > 2), or decreased (signal log ratio change < 2), or marginally increased or decreased. We used DAVID, an online bioinformatics tool designed to identify several genes or protein functions [22,23], to visualize KEGG pathways (Kyoto Encyclopedia of Genes and Genomes, a database resource that integrates genomic, chemical, and systemic functional information) enriched by the TB-upregulated genes.

2.4. Immunohistochemical analysis and immunofluorescence microscopy

For immunohistology, inguinal WAT was fixed in 4% paraformaldehyde solution and embedded in paraffin. Paraffin sections of 4 μm thickness were dewaxed and incubated with rabbit anti-UCP1 antibody (GeneTex, Irvine, CA) in PBS containing 3% BSA and immunostaining was performed using a peroxidase staining 3,3′-diaminobenzidine (DAB) kit (Nacalai Tesque, Kyoto, Japan). For immunofluorescence microscopy of ASCs, the cells were cultured on coverslips in 24 well plates. The adipocytes were incubated in the presence of 100 nM MitoBright Red (Dojindo Molecular Technologies, Inc., Kumamoto, Japan) for 60 min, and then cells were fixed by using 4% paraformaldehyde solution and permeabilized with 0.1% Triton X-100 in PBS. Subsequently, the cells were treated with PBS containing 10% FBS, 5% BSA, and 0.1% sodium azide, and then incubated with primary anti-UCP1 or anti-LC3 (MBL, Nagoya, Japan) antibody in PBS containing 3% BSA, followed by incubation with Alexa Fluor 488-conjugated secondary anti-rabbit IgG. Nuclei were stained with Hoechst 33258 (1 μg/mL; Nacalai Tesque) at 23±2℃ for 20 min. The intensity of each fluorescent signal was quantified using ImageJ

software (National Institutes of Health, Bethesda, MD), and the ratio of each signal level was normalized to that of the Hoechst 33258 (Nuclei marker) level. Tissue sections and cells were imaged with a confocal laser scanning microscope (FV1000-D; Olympus Optical Co. Ltd., Tokyo, Japan). Adipocyte sizes were calculated from more than 300 cells in each group using the measurement tool in ImageJ software.

2.5. Western blotting

Cell lysate preparation and western blotting were performed as previously described [20]. In brief, the cells and adipose tissues were lysed and homogenized in the lysis buffer, respectively. The lysates were then subjected to SDS-PAGE and analyzed by western blotting using the following mouse mAb: anti-GAPDH (clone; 5A12, Fujifilm Wako, Osaka, Japan) and rabbit polyclonal [anti-ATG3 (GeneTex, Irvine, CA), anti-COXIV (Proteintech, Chicago, IL), anti-LC3, anti-p62 (Cell Signaling Technology), and anti-UCP1 antibodies]. The immunoreactive complexes were detected with the LAS500 (GE healthcare). The intensity of each band was quantified using ImageJ, and the ratio of each protein level was normalized to that of the GAPDH (loading control) level.

2.6. Quantitative real-time PCR (qPCR)

Total RNA was extracted from inguinal WAT and ASCs using Sepal-RNA II Super (Nacalai Tesque) according to the manufacturer's instructions, and cDNAs were synthesized. qPCR was performed with KAPA SYBER FAST qPCR Master Mix

(NIPPON Genetics, Kyoto, Japan) using the specific primers (see Supplementary Table S1). The relative expression levels of each gene were calculated using the $2^{-\Delta\Delta Ct}$ (CT, cycle threshold) method, and data were normalized to the expression level of *Gapdh*, which was used as an endogenous control.

2.7. Oxygen consumption rate (OCR)

The extracellular OCR was measured using Oxygen Consumption Rate Assay Kit (Cayman Chemical, MI, USA) according to the manufacturer's instructions. ASCs were grown to confluence and differentiated into mature adipocytes with or without TB (5 μM) in the presence or absence of rosiglitazone (10 μM) for 7 days in 96-well culture plates. The spent culture medium was replaced with fresh DMEM supplemented with high glucose. To calculate basal respiration, proton leak, and ATP production rate, the cells were incubated with 1.5 μM oligomycin or 1 μM antimycin A for 90 min. Fluorescence (excitation at 380 nm; emission at 630 nm) of phosphorescent oxygen probe was measured using a multi-detection microplate reader (Powerscan HT; Dainippon Pharmaceutical, Osaka, Japan).

2.8. Luciferase reporter assay

The transcriptional activity of PPARγ was measured by transiently transfecting cells with reporter vectors [p3×PPRE-Luc and pRL-SV40 (control reporter vector; Promega)] and Myc-PPARγ expression vector (pLVSIN-Myc-PPARγ). Signal activities of the β3-

adrenergic receptor (β3-AR) were measured by using transfection with CRE-responsive reporter vector (p6×CRE-Luc) and β3-AR expression vectors (pLVSIN-Myc-β3-AR). After transfection, the cells were incubated with 5 μM TB for 24 h. Firefly and Renilla luciferase activities were measured using the Dual-Luciferase reporter assay kit and GloMax 20/20 Luminometer (Promega). Transfection efficiency was normalized to that of Renilla luciferase. Data are expressed as relative light units (RLU; firefly levels divided by Renilla levels).

2.9. Isolation of phosphorylated proteins and immunoprecipitation

Phosphorylated proteins in ASCs were isolated using Phos-tag agarose (Fujifilm Wako) according to the manufactures' instructions. Briefly, the cells were lysed with lysis buffer, and the cell lysates (15 μg proteins) were incubated with 40 μL of Phos-tag agarose (50% slurry: Fujifilm Wako) for affinity-purification of phosphorylated proteins. The resin was washed, and protein bound to the resin was subjected to SDS-PAGE, followed by western blot analysis. Immunoprecipitation was performed as previously described [24]. In brief, the cell lysates were incubated with unimmunized control IgG or mouse monoclonal anti-PPARγ IgG, followed by incubation with 40 μL protein G-Sepharose resin (80% slurry; GE Healthcare) at 4℃ for 1 h. The resin was washed, and proteins bound to the resin were separated by SDS-PAGE and analyzed by western blotting.

2.10. Statistical analysis

Data were analyzed by one- or two-way analysis of variance with Tukey's post hoc testing. Statistical analysis was performed with JMP statistical software version 11.2.0 (SAS Institute. Cary, NC). *In vivo* and *in vitro* data are expressed as means ± SEM and ± SD, respectively. A p-value of < 0.05 was considered statistically significant.

3. Results

3.1. Dietary TB decreases weight gain and increases skin temperature

We investigated the effect of TB administration on the accumulation of body fat in mice. The dietary intake of TB decreased the weight gain of the mice in the 0.1% TB group compared to the mice in the control group. In addition, the final body weight was smaller in the 0.1% TB group than in the control group ($p = 0.067$; Fig. 1A). To determine the effects of TB intake on body temperature, the skin temperature of the inguinal region was measured by using an infrared thermography camera, which revealed that TB significantly increased skin temperature of the inguinal region in mice of the 0.1% TB group (Fig. 1B). No difference in skin temperature was observed between the control group and the 0.05% TB group. Therefore, the subsequent analysis mainly compared the control group and the 0.1% TB group.

At the end of the experiment, we collected inguinal adipose tissue as subcutaneous WAT, perigonadal and retroperitoneal adipose tissues as visceral WAT and interscapular adipose tissue was collected as BAT. The adipose tissue weights of inguinal and retroperitoneal regions were lower in the 0.1% TB group than that in the control group

(Fig. 1C). In contrast, TB did not affect adipose tissue weight of perigonadal WAT and interscapular BAT. Furthermore, the NEFA levels were attenuated in the 0.1% TB group (Fig. 1D), whereas the average daily energy intake during the 63 days was not influenced by TB intake (Fig. 1E). These results indicate that dietary intake of 0.1% TB decreased the weight gain of WAT and increased skin temperature in mice.

3.2. Dietary TB induces expression of thermogenic proteins and miniaturization of adipocytes in subcutaneous WAT

The induction of UCP1 protein expression and adipocyte miniaturization are the characteristic feature of the browning of WAT. Therefore, we examined the effect of TB intake on the expression levels of UCP1 protein and mitochondrial marker protein in each adipose tissue. The results demonstrated that TB intake significantly induced UCP1 protein in inguinal WAT of mice in the 0.1% TB group, whereas the protein expression of UCP1 was not detected in the WAT of the mice in the control group (Fig. 2A). Furthermore, the mitochondrial marker protein COXIV levels were increased in inguinal and perigonadal WAT in the 0.1% TB group than that in the control group. However, the dietary intake of TB did not change the protein levels of UCP1 and COXIV in BAT among the three groups. The protein induction of UCP1 and COXIV was also obtained by dietary 0.2% TB intake (Supplementary Fig. S1). Immunohistochemical staining showed that the UCP1-immunopositive area was distinctly expanded in inguinal WAT of the 0.1% TB group (Fig. 2B), whereas it did not affect the UCP1-immunopositive area in perigonadal adipose tissues. Furthermore, we quantified the effect of dietary supplementation of TB

on the adipocyte size and demonstrated that the 0.1% TB group had smaller adipocytes with a reduction in mean adipocyte area than those in the control group (Fig. 2C). In addition, the frequency distribution of adipocyte size was shifted toward a smaller size in TB-supplemented mice than in control mice (Fig. 2D). These results indicate that TB intake induces the UCP1 expression in subcutaneous WAT but not in visceral WAT. In addition, it induces healthy expansion of WAT through adipocyte hyperplasia by increasing the number of small and healthy adipocytes.

3.3. TB changes gene expression profile for browning of subcutaneous WAT

To determine whether TB affects transcriptomic changes for other browning-associated genes in inguinal WAT, we performed the genome-wide analysis using GeneChip assay. It identified that 636 genes were significantly differentially expressed (fold change > 2 or < 0.5) in inguinal WAT between the control and 0.1% TB groups (Supplementary Table S2). These differentially expressed genes included the genes involved in brown cell differentiation and beige adipocyte markers (Table 1). TB increased the expression of *Ucp1* and browning-associated genes, such as *Elovl3*, *Cidea*, *Cox7a1*, *Cox8b*, and *Cpt1b* in inguinal WAT, and similar results were obtained by qPCR (Fig. 3A), whereas some other browning-associated genes, such as *Prdm16*, *Ppargc1a*, *Ppargc1b*, were largely unchanged by TB intake (Supplementary Table S2). To understand the possible pathway of TB-upregulated genes, KEGG pathway enrichment was re-analyzed using DAVID Bioinformatics Resources. Results showed that six genes (*UCP1*, *FABP3*, *CPT-1*, *FATP1/4*, *FABP*, and *FATP*) were markedly enriched in the PPAR signaling pathway. In

328 particular, four genes (*UCP1*, *FABP3*, *CPT-1* and *FATP1/4*) are downstream of PPARγ
329 (Supplementary Fig. S2). However, TB suppressed the expression levels of PPARγ target
330 genes such as *Fabp4*, *Cd36*, and *Lep* in WAT (Fig. 3B), whereas PPARγ levels were not
331 affected by TB intake (Fig. 3B and 3C). These results indicate that TB induces WAT
332 browning at transcriptional levels and suggests that PPARγ is involved in TB-induced
333 browning.
334
335 *3.4. Direct effect of TB treatment on browning-associated genes in mice primary*
336 *adipocytes*
337
338 From the *in vivo* experiments, it was unclear whether TB induces the browning of white
339 adipocytes by directly stimulating the preadipocytes. Therefore, we analyzed the direct
340 effect of TB on white adipocyte browning using primary culture cells; we prepared
341 adipose stromal cells (ASCs) capable of differentiating into brown adipocytes from
342 inguinal WAT. The results showed that TB alone did not influence UCP1 protein levels
343 in ASCs; however, in combination with rosiglitazone, a synthetic PPARγ ligand, it
344 increased UCP1 protein levels (Fig. 4A). In addition, COXIV protein levels were also
345 synergistically increased by TB and rosiglitazone, and the increase in UCP1 and COXIV
346 proteins demonstrated a dose-dependency (Fig. 4B). Moreover, the protein levels of
347 PPARγ and PRDM16 were increased by rosiglitazone, whereas TB did not influence these
348 protein levels. Furthermore, the expression level of the *Ucp1* gene was also
349 synergistically enhanced by TB in the presence of rosiglitazone (Fig. 4C and 4D). In
350 addition, it also upregulated the expression of browning-associated genes (Fig. 4E). On

the contrary, TB did not influence the expression of PPARγ target genes such as *Fabp4* and *Cd36* in WAT. These results indicate that TB induces browning of ASCs in a PPARγ activation-dependent manner.

3.5. Effect of TB on proton leak in mitochondria

Based on the findings that TB enhanced UCP1 expression in a rosiglitazone concentration-dependent manner, we hypothesized that TB might change uncoupled OCR from proton leak in the mitochondrial respiration. To prove our hypothesis, OCR was measured in differentiated ASCs using oligomycin, an inhibitor of ATP synthase, and antimycin, an inhibitor of the mitochondrial electron transport chain. Rosiglitazone elevated basal OCR and uncoupled OCR from proton leak, which were further enhanced by TB (Fig. 5 *left panel and middle panel*). On the contrary, TB had no influence on ATP-generating OCR in the presence of rosiglitazone (Fig. 5, *right panel*). Our results indicate that TB enhances mitochondrial uncoupling respiration in parallel with increased UCP1 protein levels in a PPARγ activation-dependent manner.

3.6. Direct effect of TB treatment on browning-associated factors

The ligand-bound PPARγ and β3-AR induce adipocyte browning of white adipocyte, respectively. Therefore, it is expected that TB could act as a PPARγ or β3-AR agonist. To test this possibility, we analyzed the PPARγ and β3-AR-mediated transcriptional activity of TB. The results showed that TB did not influence PPARγ transactivation and β3-AR-

374 mediated transcriptional activity (Fig. 6A and 6B), suggesting that TB enhances PPARγ
375 signaling; however, it does not act as a PPARγ ligand.
376
377 *3.7. TB promotes phosphorylation of PGC-1α*
378
379 Next, we investigated the effect of TB on the status of PGC-1α in ASCs. Although TB
380 slightly increased the gene expression of *Ppargc1a*, its protein (PGC-1α) levels did not
381 increase (Fig. 7A and 7B), whereas rosiglitazone neither influenced the expression of the
382 *Ppargc1a* gene nor its protein and mRNA levels. Subsequently, to determine whether TB
383 affects the phosphorylation of PGC-1α, the phosphorylated proteins were affinity-
384 purified from TB-treated ASCs using Phos-tag agarose, and PGC-1α was detected with
385 western blotting. The overall phosphorylation level of PGC-1α was increased by TB in
386 the presence of rosiglitazone, but not by rosiglitazone alone (Fig. 7C). Furthermore, co-
387 immunoprecipitation showed that TB increased the interaction with PPARγ and PGC-1α
388 in the presence of rosiglitazone (Fig. 7D). These results suggest that TB enhances PPARγ
389 activation by regulation of PGC-1α phosphorylation levels.
390
391 *3.8. TB increases mitochondria mass through inhibition of mitophagy*
392
393 Fluorescence staining of mitochondria with MitoBright revealed that rosiglitazone
394 increased MitoBright-positive areas in ASCs, whereas TB enhanced the effect of
395 rosiglitazone on mitochondrial mass (Fig. 8A). Furthermore, like MitoBright, the
396 fluorescent area of UCP1 in mitochondria was expanded by TB in the presence of

rosiglitazone, indicating the synergistic effects of TB and rosiglitazone on mitochondria mass. As mitochondria mass is regulated by biogenesis and mitophagy, the specific autophagic elimination of mitochondria [25], we investigated the influence of TB on the expression levels of mitochondrial biogenesis-associated genes, such as *Tfam*, *Nrf1*, and *Cycs*. The results demonstrated no significant influence of TB on the expression of these genes (Fig. 8B). Similarly, to determine whether TB regulates mitophagy, we assessed the autophagosome marker LC3 in TB-treated ASCs and observed a decrease in the conversion ratio of LC3-I to LC3-II in a dose-dependent manner (Fig. 8C). These findings indicate the suppression of autophagy. Furthermore, the autophagy adaptor protein p62 and autophagy-related 3 (ATG3) were accumulated in TB-treated ASCs, while these gene expression levels were not increased by TB (Fig. 8D), indicating that TB suppresses protein degradation of p62 and ATG3 by autophagy. Furthermore, immunofluorescence microscopy revealed the formations of LC3-II-derived punctate structures in ASCs, which were attenuated by TB treatment (Fig. 8E). These results indicate that TB increases mitochondria mass through the suppression of mitophagy.

4. Discussion

The activation of brown and beige adipocytes can prevent obesity and its-associated diseases by increasing thermogenesis and improving lipid and carbohydrate metabolism. In humans, brown adipocytes are abundant in newborns; whereas, they decrease significantly with growth. However, the beige adipocyte in adult humans plays a similar role in BAT. Furthermore, they exhibit a similar genotype as that of mouse beige

adipocytes [26], indicating that induction of transformation of beige adipocytes from white adipocytes in mice could be applied to human researches. In addition, it has also been shown that the thermogenic activity of inducible beige adipocytes is higher than that of brown adipocytes [27]. Therefore, the induction of white adipocyte browning has more potential as a therapeutic strategy for obesity and its associated diseases. Several studies have attempted to induce browning by chemical materials; however, due to the adverse side effects of the chemicals, the research interests in nutraceuticals have increased. In this study, we made a concerted effort to show the efficacies of TB, a natural alkaloid found in cocoa. The findings demonstrated that TB induces the development of beige adipocytes in inguinal WAT in mice. Furthermore, our data indicate that PPARγ signaling is essential for TB-mediated induction of beige adipocyte differentiation in primary culture cells.

Several studies have reported that the chemical molecules activate thermogenesis and directly or indirectly induces adipocyte browning via various signaling pathways [28–30]. However, dietary foods, such as curcumin, capsaicin, fish oil, etc., which are rich in eicosatetraenoic acid and docosahexaenoic acid, induce WAT browning via the sympathetic nervous system (SNS) [28–30]. These food-derived bioactive components activate SNS by binding to transient receptor potential vanilloid 1 (TRPV1), which subsequently stimulates the release of norepinephrine, a catecholamine [28–30]. The released norepinephrine then induces white adipocyte browning by binding to β3-AR on adipocytes. Although the β3-AR signaling is a dominant pathway to activate thermogenesis in beige adipocytes and brown adipocytes, β3-AR agonists have been shown to have clinical side effects of cardiovascular diseases [31]. Here, we demonstrated

443 that TB did not stimulate β3-AR signaling in β3-AR-overexpressed adipocytes (Fig. 6B),
444 indicating that TB could be a valuable food-derived compound that induces adipocyte
445 browning by directly stimulating adipocytes in a β3-AR-independent manner.
446 The findings also revealed that TB enhanced UCP1 protein levels in primary culture
447 cells in a PPARγ activation-dependent manner. PPARγ is required to differentiate white
448 and brown adipocytes, while overexpression of PPARγ is not sufficient for the browning
449 of white adipocytes [32], indicating that the activation of PPARγ by its agonists is
450 required for browning of white adipocytes. Moreover, the ability of PPARγ agonists to
451 induce UCP1 has also been documented [8,9,12]. Studies have also shown that PPARγ
452 synergistically promotes UCP1 expression and adipocyte browning by coordinating with
453 other factors, such as the fibroblast growth factor 21 (FGF21), a predominant liver-
454 derived hormone that regulates lipid and glucose homeostasis. Subcutaneous injection of
455 FGF21 increases *Ucp1* expression and promotes WAT [33]; however, direct treatment to
456 culture cells (preadipocyte or adipocyte) hardly increases *Ucp1* expression [34].
457 Interestingly, the combination of FGF21 and PPARγ agonist has been shown to
458 synergistically increase *Ucp1* expression, indicating that FGF21 can induce browning of
459 adipocytes, but only with PPARγ activation [34]. The increase in UCP1 protein levels
460 demonstrated in this study by TB is similar to the effect of FGF21 in a PPARγ activation-
461 dependent manner.
462 Furthermore, our results revealed that TB increased the phosphorylation of PGC-1α;
463 however, it had no influence on the PGC-1α protein level (Fig. 7B). Although PGC-1α is
464 not required for adipocyte differentiation, it is essential for cold- or β3-AR agonist-
465 induced thermogenic gene expression in WAT [35]. Reportedly, PGC-1α expression and

activity are regulated by p38 mitogen-activated protein kinase in response to β3-AR agonist, and β3-AR signaling-induced phosphorylation of PGC-1α regulates the thermogenic gene expression through interaction with PPARγ in brown adipocytes [13]. Furthermore, the activation of AMP-activated kinase in skeletal muscle increases glucose uptake and gene expression of UCP2, UCP3 by the phosphorylation of PGC-1α [36]. Taken together, these results indicate that TB synergistically enhances UCP1 expression and adipocyte browning by coordinating with PPARγ, and the increased phosphorylation of PGC-1α by TB regulates the PPARγ-mediated UCP1 expression.

TB further enhanced the rosiglitazone-induced elevation in basal respiration and proton leak. Reportedly, increased protein expression of UCP1 promotes uncoupling respiration from proton leak [2]. Furthermore, it has also been shown that rosiglitazone and β-adrenergic stimulation enhances the expression of UCP1 protein and mitochondrial respiration, including basal respiration and uncoupling respiration, wherein *UCP1* knockdown decreased the rosiglitazone-induced increase in uncoupling respiration in adipocytes [37], indicating that UCP1 plays an important role in the regulation of uncoupling respiration by PPARγ activation. Concordant with these findings, our findings demonstrated a similar mechanism of increase in mitochondrial uncoupling respiration by TB is mediated via an increased expression of UCP1 in adipocytes. UCP1-mediated uncoupling respiration is known to generate heat. It has been shown that food-derived bioactive compounds that promote the browning of WAT improve cold tolerance by increasing the expression of thermogenic genes that generates heat [38]. Consistent with this study findings, our data provide evidence that TB intake increases UCP1 protein levels in subcutaneous WAT and skin temperature in mice (Fig. 1B and 2A), suggesting

that it might play a role in adaptation to cold; however, further studies are required to explore this aspect of TB and its underlying mechanisms.

TB decreased the conversion of LC3-I to LC3-II, an autophagy marker, in a dose-dependent manner, indicating that autophagy is suppressed by TB. It has been shown that mitochondrial degradation by mitophagy is involved in decreasing beige adipocytes, and the activation of autophagy has been observed in adipose tissue of obese individuals [39]. Furthermore, the knockout of the autophagy-related gene *Atg7* has been shown to increase the mitochondrial mass and brown-like adipocyte in WAT and protect from diet-induced obesity [40,41]. In addition, pharmacological inhibition of mitophagy has been reported to maintain the functional beige adipocytes even after withdrawal of the browning stimuli [40]. In contrast, browning stimuli also increase the mitochondrial mass by inducing mitochondrial biogenesis regulators, such as *PGC-1α, Nrf1*, and *Tfam* [25]. However, TB did not influence the expression levels of these transcriptional regulators (Fig. 8B). Interestingly, Altshuler-Keylin et al. (2016) reported that mitochondrial biogenesis contributes to the maintenance of high mitochondrial mass in brown adipocytes, while down-regulation of mitophagy plays a critical role in the mitochondrial homeostasis in beige adipocytes [42]. Taken together, our results suggest that TB increases mitochondrial mass and maintains the characteristic of brown-like adipocytes by down-regulation of mitophagy.

In this study, we treated the ASCs with rosiglitazone, a synthetic PPARγ agonist, to selectively activate PPARγ. Several studies have reported that the endogenous ligands for PPARγ include long-chain fatty acids and prostanoids with low binding affinities do not activate PPARγ signaling at their physiological concentrations [12,43,44]. In contrast,

512 Baker et al. (2005) and Schopfer et al. (2005) found nitroalkene derivatives of unsaturated
513 fatty acid (nitrolinoleic acid and nitrooleic acid) in human plasma serve as strong
514 endogenous PPARγ ligands [45,46]. Like rosiglitazone, nitrolinoleic acid activates
515 PPARγ at physiological concentrations and exhibits antidiabetic and antiadipogenic
516 effects *in vivo* [46,47]. Our results showed that TB induced browning of WAT even
517 without administration of rosiglitazone *in vivo*, indicating that TB might promote
518 browning of WAT by interacting with the activation of PPARγ and could serve a potent
519 endogenous ligand *in vivo*.

520 The effects of nutraceuticals derived from the bioactive components of food vary
521 depending on their concentration. For example, it has been reported that the daily intake
522 of a high dose of TB tends to result in higher blood concentrations, and in the human
523 intervention studies with TB, its blood concentrations increase to about 28.75 μM [48].
524 We have previously demonstrated that a high concentration of TB (25 μM) suppresses
525 adipogenesis and adipocyte differentiation in 3T3-L1 adipocytes and younger mice. It
526 also reduces the expression of PPARγ [20]. In addition, another study has reported that
527 adipogenesis is decreased by high concentrations of TB {150 μg/mL (877 μM)} [49].
528 Here, we show that UCP1 is upregulated by TB at a concentration of 5 μM, indicating
529 that a low concentration of TB affects white adipocytes browning but not adipogenesis
530 and PPARγ protein levels. Collectively, these results suggest that TB could exert different
531 effects depending on its concentration.

532 The present results demonstrate that TB directly induces adipocyte browning; however,
533 the target proteins to which TB binds to induce adipocyte browning are elusive.
534 Methylxanthine compounds, including TB, caffeine, and theophylline, play as antagonists

of the adenosine receptor (AR) family. ARs regulate adipogenesis, lipolysis, and adipocyte browning, whereas AR1 and AR2a show contrasting actions in adipocytes [50]. In WAT, AR1 agonist inhibits lipolysis, followed by a greater capacity for thermogenesis and activation of UCP1 [51], and knockout or pharmacological inhibition of AR1 increases lipolysis in white adipocytes of mice [52]. On the contrary, AR2a agonist increases UCP1 expression and induces adipose browning without affecting norepinephrine production [52]. Previously we have shown that TB exerts an anti-adipogenic effect by interaction with AR1, but not with AR2a in 3T3-L1 adipocyte [20]. These results suggest that TB inhibits the function of AR1 by binding to it as an antagonist, resulting in the activation of AR2a, which in turn promotes UCP1 expression and adipose browning. However, for precise identification of the target proteins and to clarify the exact molecular mechanism of TB-induced browning, further studies are warranted.

In summary, this is the first study to show that TB intake induces UCP1 and thermogenesis in subcutaneous WAT *in vivo* and enhances PPARγ signaling *in vitro*. These data provide evidence that dietary intervention of TB could be useful in inducing adipocyte browning and assist in developing a potential therapeutic strategy for the prevention of obesity and its associated diseases.

Acknowledgments

This work was supported by JSPS KAKENHI (grant number: 18K14405) for scientific research (to T.M.) and by encouraging research grants (to T.M.) from the LOTTE foundation. The protein detection, immunofluorescent microscopy, and qPCR analysis were conducted at Research Center for Supports to Advanced Science, Shinshu

University. We would like to thank Editage (www.editage.jp) for English language editing (JOB CODE; ZUMIT_5).

Author Contributions

Emi Tanaka: Conceptualization, Methodology, Investigation, Formal analysis, Writing - Review & Editing. Takakazu Mitani: Conceptualization, Methodology, Writing - Original Draft, Writing - Review & Editing. Momona Nakashima: Investigation, Formal analysis. Eito Yonemoto: Investigation, Formal analysis. Fujii Hiroshi: Resources, Investigation, Formal analysis. Hitoshi Ashida: Formal analysis.

Conflicts of Interest

The authors declare that there are no conflicts of interest.

References

[1] Kahn SE, Hull RL, Utzschneider KM. Mechanisms linking obesity to insulin resistance and type 2 diabetes. Nature 2006;444:840–6.

[2] Kajimura S, Spiegelman BM, Seale P. Brown and beige fat: physiological roles beyond heat generation. Cell Metab 2015;22:546–59.

[3] Cypess AM, Lehman S, Williams G, Tal I, Rodman D, Goldfine AB, et al. Identification and importance of brown adipose tissue in adult humans. N Engl J Med 2009;360:1509–17.

[4] Frontini A, Cinti S. Distribution and development of brown adipocytes in the murine and human adipose organ. Cell Metab 2010;11:253–6.

581 [5] Harms M, Seale P. Brown and beige fat: development, function and therapeutic
582 potential. Nat. Med 2013;19:1252–63.
583 [6] Bartesaghi S, Hallen S, Huang L, Svensson PA, Momo RA, Wallin S, et al.
584 Thermogenic activity of UCP1 in human white fat-derived beige adipocytes. Mol
585 Endocrinol 2015;29:130–9.
586 [7] L. Sidossis, S. Kajimura. Brown and beige fat in humans: thermogenic adipocytes
587 that control energy and glucose homeostasis. J Clin Invest 2015;125:478–86.
588 [8] Petrovic N, Walden TB, Shabalina IG, Timmons JA, Cannon B. Nedergaard J.
589 Chronic peroxisome proliferator-activated receptor γ (PPARγ) activation of
590 epididymally derived white adipocyte cultures reveals a population of
591 thermogenically competent, UCP1-containing adipocytes molecularly distinct from
592 classic brown adipocytes. J Biol Chem 2010;285:7153–64.
593 [9] Fukui Y, Masui S, Osada S, Umesono K, Motojima K. A new thiazolidinedione,
594 NC-2100, which is a weak PPAR-γ activator, exhibits potent antidiabetic effects
595 and induces uncoupling protein 1 in white adipose tissue of KKAy obese mice.
596 Diabetes 2000;49:759–67.
597 [10] Rong JX, Qiu Y, Hansen MK, Zhu L, Zhang V, Xie M, et al. Adipose mitochondrial
598 biogenesis is suppressed in db/db and high-fat diet-fed mice and improved by
599 rosiglitazone. Diabetes 2007;56:1751–60.
600 [11] Seale P, Conroe HM, Estall J, Kajimura S, Frontini A, Ishibashi J, et al. Prdm16
601 determines the thermogenic program of subcutaneous white adipose tissue in mice.
602 J Clin Invest 2011;121:96–105.
603 [12] Ohno H, Shinoda K, Spiegelman BM, Kajimura S. PPARγ agonists induce a white-

604 to-brown fat conversion through stabilization of PRDM16 protein. Cell Metab
605 2012;15:395–404.
606 [13] Cao W, Daniel KW, Robidoux J, Puigserver P, Medvedev AV, Bai X, et al. p38
607 mitogen-activated protein kinase is the central regulator of cyclic AMP-dependent
608 transcription of the brown fat uncoupling protein 1 gene. Mol Cell Biol
609 2004;24:3057–67.
610 [14] Nissen SE, Wolski K. Effect of rosiglitazone on the risk of myocardial infarction
611 and death from cardiovascular causes. N Engl J Med 2007;356:2457–71.
612 [15] Shively CA, Tarka Jr SM. Methylxanthine composition and consumption patterns
613 of cocoa and chocolate products. Prog Clin Biol Res 1984;158:149–78.
614 [16] Barrera-Reyes PK, Hernández-Ramírez N, Cortés J, Poquet L, Redeuil K, Rangel-
615 Escareño C, et al. Gene expression changes by high-polyphenols cocoa powder
616 intake: a randomized crossover clinical study. Eur J Nutr 2019;58:1887–98.
617 [17] Taubert D, Roesen R, Lehmann C, Jung N, Schömig E. Effects of low habitual
618 cocoa intake on blood pressure and bioactive nitric oxide: a randomized controlled
619 trial. JAMA 2007;298:49–60.
620 [18] Wan Y, Vinson JA, Etherton TD, Proch J, Lazarus SA, Kris-Etherton PM. Effects of
621 cocoa powder and dark chocolate on LDL oxidative susceptibility and
622 prostaglandin concentrations in humans. Am J Clin Nutr 2001;74:596–602.
623 [19] Yamashita Y, Mitani T, Wang L, Ashida H. Methylxanthine derivative-rich cacao
624 extract suppresses differentiation of adipocytes through downregulation of PPARγ
625 and C/EBPs. J Nutr Sci Vitaminol 2018;64:151–60.
626 [20] Mitani T, Watanabe S, Yoshioka Y, Katayama S, Nakamura S, Ashida H.

627 Theobromine suppresses adipogenesis through enhancement of CCAAT-enhancer-
628 binding protein β degradation by adenosine receptor A1. Biochim Biophys Acta
629 Mol Cell Res 2017;1864:2438–48.
630 [21] Wang Y, Sato M, Guo Y, Bengtsson T, Nedergaard J. Protein kinase a-mediated cell
631 proliferation in brown preadipocytes is independent of Erk1/2, PI3K and mTOR.
632 Exp Cell Res 2014;328:143–55.
633 [22] Huang DW, Sherman BT, Lempicki RA. Systematic and integrative analysis of
634 large gene lists using DAVID bioinformatics resources. Nat Protoc 2009;4:44–57.
635 [23] Huang DW, Sherman BT, Lempicki RA. Bioinformatics enrichment tools: paths
636 toward the comprehensive functional analysis of large gene lists. Nucleic Acids Res
637 2009;37:1–13.
638 [24] Mitani T, Harada N, Nakano Y, Inui H, Yamaji R. Coordinated action of hypoxia-
639 inducible factor-1α and β-catenin in androgen receptor signaling. J Biol Chem
640 2012;287:33594–606.
641 [25] Altshuler-Keylin S, Kajimura S. Mitochondrial homeostasis in adipose tissue
642 remodeling. Sci Signal 2017;10:eaai9248.
643 [26] Sharp LZ, Shinoda K, Ohno H, Scheel DW, Tomoda E, Ruiz L, et al. Human BAT
644 possesses molecular signatures that resemble beige/brite cells. PLoS One
645 2012;7:e49452.
646 [27] Okamatsu-Ogura Y, Fukano K, Tsubota A, Uozumi A, Terao A, Kimura K, et al.
647 Thermogenic ability of uncoupling protein 1 in beige adipocytes in mice. PLoS One
648 2013;8:e84229.
649 [28] Nishikawa S, Kamiya M, Aoyama H, Nomura M, Hyodo T, Ozeki A, et al. Highly

650 dispersible and bioavailable curcumin but not native curcumin induces brown-like
651 adipocyte formation in mice. Mol Nutr Food Res 2018;62:doi:
652 10.1002/mnfr.201700731.
653 [29] Ohyama K, Nogusa Y, Shinoda K, Suzuki K, Bannai M, Kajimura S. A synergistic
654 antiobesity effect by a combination of capsinoids and cold temperature through
655 promoting beige adipocyte biogenesis. Diabetes 2016;65:1410–23.
656 [30] Kim M, Goto T, Yu R, Uchida K, Tominaga M, Kano Y, et al. Fish oil intake
657 induces UCP1 upregulation in brown and white adipose tissue via the sympathetic
658 nervous system. Sci Rep 2015;5:18013.
659 [31] Villarroya F, Vidal-Puig A. Beyond the sympathetic tone: the new brown fat
660 activators. Cell Metab 2013;17:638–43.
661 [32] Sugii S, Olson P, Sears DD, Saberi M, Atkins AR, Barish GD, et al. PPARγ
662 activation in adipocytes is sufficient for systemic insulin sensitization. Proc Natl
663 Acad Sci U S A 2009;106:22504–9.
664 [33] Fisher FM, Kleiner S, Douris N, Fox EC, Mepani RJ, Verdeguer F, et al. FGF21
665 regulates PGC-1α and browning of white adipose tissues in adaptive thermogenesis.
666 Genes Dev 2012;26:271–81.
667 [34] Kroon T, Harms M, Maurer S, Bonnet L, Alexandersson I, Lindblom A, et al.
668 PPARγ and PPARα synergize to induce robust browning of white fat in vivo. Mol
669 Metab 2020, 36, 100964.
670 [35] Leone TC, Lehman JJ, Finck BN, Schaeffer PJ, Wende AR, Boudina S, et al. PGC-
671 1α deficiency causes multi-system energy metabolic derangements: muscle
672 dysfunction, abnormal weight control and hepatic steatosis. PLoS Biol

673 2005;3:e101.
674 [36] Jäger S, Handschin C, St-Pierre J, Spiegelman BM. AMP-activated protein kinase
675 (AMPK) action in skeletal muscle via direct phosphorylation of PGC-1α. Proc Natl
676 Acad Sci U S A 2007;104:12017–22.
677 [37] Nicole WMK, Michael MS, Jenny EG. Inducible UCP1 silencing: A lentiviral
678 RNA-interference approach to quantify the contribution of beige fat to energy
679 homeostasis. PLoS One 2019;14:e0223987.
680 [38] Shan W, Xiuchao W, Zichen Y, Chengming X, Ming Z, Banjun R, et al. Curcumin
681 promotes browning of white adipose tissue in a norepinephrine-dependent way.
682 Biochem Biophys Res Commun 2015;466:247–53.
683 [39] Jansen HJ, van Essen P, Koenen T, Joosten LAB, Netea MG, Tack CJ, et al.
684 Autophagy activity is up-regulated in adipose tissue of obese individuals and
685 modulates proinflammatory cytokine expression. Endocrinology 2012;153:5866–
686 74.
687 [40] Singh R, Xiang Y, Wang Y, Baikati K, Cuervo AM, Luu YK, et al. Autophagy
688 regulates adipose mass and differentiation in mice. J Clin Invest 2009;119:3329–39.
689 [41] Zhang Y, Goldman S, Baerga R, Zhao Y, Komatsu M, Jin S. Adipose-specific
690 deletion of autophagy-related gene 7 (atg7) in mice reveals a role in adipogenesis.
691 Proc Natl Acad Sci U S A 2009;106:19860–5.
692 [42] Altshuler-Keylin S, Shinoda K, Hasegawa Y, Ikeda K, Hong H, Kang Q, et al.
693 Beige adipocyte maintenance is regulated by autophagy-induced mitochondrial
694 clearance. Cell Metab 2016;24:402–19.
695 [43] Tzameli I, Fang H, Ollero M, Shi H, Hamm JK, Kievit P, et al. Regulated

696 production of a peroxisome proliferator-activated receptor-gamma ligand during an
697 early phase of adipocyte differentiation in 3T3-L1 adipocytes. J Biol Chem
698 2004;279:36093–102.
699 [44] Bell-Parikh LC, Ide T, Lawson JA, McNamara P, Reilly M, FitzGerald GA.
700 Biosynthesis of 15-deoxy-delta12,14-PGJ2 and the ligation of PPARγ. J Clin Invest
701 2003;112:945–55.
702 [45] Baker PRS, Lin Y, Schopfer FJ, Woodcock SR, Groeger AL, Batthyany C, et al.
703 Fatty acid transduction of nitric oxide signaling: multiple nitrated unsaturated fatty
704 acid derivatives exist in human blood and urine and serve as endogenous
705 peroxisome proliferator-activated receptor ligands. J Biol Chem 2005;280:42464–
706 75.
707 [46] Schopfer FJ, Lin Y, Baker PRS, Cui T, Garcia-Barrio M, Zhang J, et al.
708 Nitrolinoleic acid: an endogenous peroxisome proliferator-activated receptor
709 gamma ligand. Proc Natl Acad Sci U S A 2005;102:2340–5.
710 [47] Schopfer FJ, Cole MP, Groeger AL, Chen CS, Khoo NKH, Woodcock SR, et al.
711 Covalent peroxisome proliferator-activated receptor gamma adduction by nitro-
712 fatty acids: selective ligand activity and anti-diabetic signaling actions. J Biol Chem
713 2010;285:12321–33.
714 [48] Neufingerl N, Zebregs YEMP, Schuring EAH, Trautwein EA. Effect of cocoa and
715 theobromine consumption on serum HDL-cholesterol concentrations: a randomized
716 controlled trial. Am J Clin Nutr 2013;97:1201–9.
717 [49] Jang YJ, Koo HJ, Sohn EH, Kang SC, Rhee DK, Pyo S. Theobromine inhibits
718 differentiation of 3T3-L1 cells during the early stage of adipogenesis via AMPK

719 and MAPK signaling pathways. Food Funct 2015;6:2365–74.
720 [50] Gharibi B, Abraham AA, Ham J, Evans BAJ. Contrasting effects of A1 and A2b
721 adenosine receptors on adipogenesis. Int J Obes 2012;36:397–406.
722 [51] Johansson SM, Lindgren E, Yang JN, Herling AW, Fredholm BB. Adenosine A1
723 receptors regulate lipolysis and lipogenesis in mouse adipose tissue-interactions
724 with insulin. Eur J Phamacol 2008;597:92–101.
725 [52] Gnad T, Scheibler S, von Kügelgen I, Scheele C, Kilić A, Glöde A, et al. Adenosine
726 activates brown adipose tissue and recruits beige adipocytes via A2A receptors.
727 Nature 2014;516:395–9.
728
729

730 **Figure legend**

731

732 **Fig. 1. Body and adipose tissue weight in theobromine (TB) treated mice.** (**A**)
733 C57BL/6J mice were administered a diet containing 0%, 0.05% or 0.1% TB. Body weight
734 was recorded for 63 days. (**B**) Skin temperature of the inguinal region. (**C**) The weight of
735 the liver and each adipose tissue of mice with TB supplementation. Ing; inguinal adipose
736 tissue, Peri; perigonadal adipose tissue, Retro; retroperitoneal adipose tissue, IS;
737 interscapular BAT. Inguinal, perigonadal, and retroperitoneal adipose tissues are
738 categorized as WAT. (**D**) Levels of plasma no-esterified fatty acid (NEFA) in mice with
739 0.1% TB supplementation. (**E**) Daily food intake for mice with 0.1% TB supplementation.
740 Data are presented as the mean ± SEM (n = 6). Statistically significant differences are
741 indicated by an asterisk (*$p < 0.05$).

742

743 **Fig. 2. Effect of dietary TB on the expression of thermogenesis and fat size in adipose**
744 **tissues.** (**A**) Protein expression of UCP1 and COXIV in WAT or BAT from mice following
745 63 days treatment with either vehicle (CTL), 0.05% TB or 0.1% TB. Western blotting
746 data shows two samples randomly selected from 5 samples in each group (*left panels*).
747 The ratio of each band was normalized to that of GAPDH. Western blotting data are
748 presented as the mean ± SEM (n = 5) (*right panels*). Inguinal, perigonadal, and
749 retroperitoneal adipose tissues are categorized as WAT. Interscapular adipose tissues are
750 categorized as BAT. (**B**) Immunohistochemical staining of UCP1 in inguinal or
751 perigonadal adipose tissues from mice following 63 days treatment with 0.1% TB. Scale
752 bar indicates 50 μm. (**C**) The average size of adipocytes was determined in the CTL and

753 0.1% TB. (**D**) Distribution of adipocytes on the transverse section was calculated (more
754 than 300 cells were measured in each group) in the CTL and 0.1% TB. Histological data
755 are presented as means ± SEM ($n = 3$). *$p < 0.05$ vs CTL.
756
757 **Fig. 3. Effect of dietary supplementation of TB on browning at gene expression levels.**
758 (**A**) The expression of browning-associated genes in inguinal WAT from mice following
759 63 days of treatment with either vehicle (CTL) or 0.1% TB. (**B**) The expression of PPARγ
760 target genes in inguinal WAT from mice. (**C**) Protein expression of PPARγ in inguinal
761 WAT of mice treated with 0.1% TB. The intensity of each band was quantified using
762 ImageJ 1.44, and the ratio of each band was normalized to that of GAPDH. Data are
763 presented as the mean ± SEM ($n = 3$), *$p < 0.05$ compared with control group.
764
765 **Fig. 4. Involvement of PPARγ in the TB-mediated expression of browning-associated**
766 **genes.** (**A**) Western blotting of UCP1 and COXIV in ASCs after induction of adipocyte
767 differentiation with a differentiation-inducing cocktail (DIC) in the presence or absence
768 of either 10 μM rosiglitazone (Rosi), 5 μM TB or both for 7 days. The intensity of each
769 band was quantified using ImageJ 1.44, and the ratio of each band was normalized to that
770 of GAPDH. n.d. (not detected). (**B**) Protein expression of UCP1 and COXIV in ASCs
771 after induction of adipocyte differentiation with the indicated concentrations of TB in the
772 presence of Rosi. The band intensity was quantified, and the ratio of each band was
773 normalized to that of GAPDH (*middle and right panels*). (**C**) Gene expression of *Ucp1*
774 in ASCs after induction of adipocyte differentiation with DIC with or without 5 μM TB
775 in the presence or absence of Rosi. (**D**) Gene expression of *Ucp1* in ASCs after induction

of adipocyte differentiation with the indicated concentrations of TB in the presence of Rosi. (**E**) Gene expression in ASCs after induction of adipocyte differentiation with or without TB in the presence of Rosi. *$p < 0.05$ compared with TB non-treated group. Data are presented as the mean ± SD ($n = 3$). Statistically significant differences are indicated by different letters ($p < 0.05$). If the groups share at least one letter between them, the difference is not statistically significant. However, if there is no common letter between the groups, the difference between them is statistically significant. All data shown are representative of triplicate independent experiments.

Fig. 5. Effect of TB on mitochondrial respiration. The OCR of from the basal respiration (*left panel*), proton leak (*middle panel*), and ATP production (*right panel*) rates were measured by using oligomycin and antimycin A in ASCs treated with 10 μM rosiglitazone (Rosi) and 5 μM TB for 7 days. Data are representative of triplicate independent experiments presented as the mean ± SD (n = 3). Statistically significant differences between the groups are indicated by different letters ($p < 0.05$). If the groups share at least one letter between them, the difference is not statistically significant. However, if there is no common letter between the groups, the difference between them is statistically significant. All data shown are representative of triplicate independent experiments.

Fig. 6. PPARγ or β3-AR ligand activity of TB. (**A**) Luciferase reporter assay for transcriptional activity of PPARγ in cells treated with 5 μM TB or 10 μM rosiglitazone (Rosi). (**B**) Luciferase reporter assay for β3-AR-mediated transcriptional activity in cells

799 treated with 5 μM TB or 100 nM CL316243, a β3-AR-selective agonist. Data are
800 presented as the mean ± SD (*n* = 3). Data are representative of triplicate independent
801 experiments presented as the mean ± SD (n = 3). Statistically significant differences
802 between the groups are indicated by different letters ($p < 0.05$).
803
804 **Fig. 7. Effect of TB on status of PGC-1α in ASCs.** (**A**) Gene expression of *Ppargc1a*
805 (PGC-1α) in ASCs after induction of adipocyte differentiation with DIC with or without
806 5 μM TB in the presence or absence of 10 μM rosiglitazone (Rosi) for 7 days. Data are
807 representative of triplicate independent experiments presented as the mean ± SD (n = 3).
808 Statistically significant differences between the groups are indicated by different letters
809 ($p < 0.05$). (**B**) Western blotting of PGC-1α in ASCs after induction of adipocyte
810 differentiation with DIC in the presence or absence of Rosi and TB. (**C**) Detection of
811 phosphorylation of PGC-1α proteins in ASCs after induction of adipocyte differentiation
812 with DIC with or without TB in the presence of Rosi. Phosphorylated proteins were pulled
813 down (PD) and analyzed by western blotting. (D) Co-immunoprecipitation of PPARγ and
814 PGC-1α in ASCs treated with or without TB in the presence of Rosi. PPARγ-interacted
815 proteins were immunoprecipitated (IP), followed by western blot analysis.
816
817 **Fig. 8. Involvement of TB in mitochondrial biogenesis and degradation**. (**A**)
818 Immunofluorescence staining of intracellular mitochondria (Red) and UCP1 (Green) in
819 ASCs after induction of adipocyte differentiation with or without 5 μM TB in the presence
820 of 10 μM rosiglitazone (Rosi). Nuclei were stained with Hoechst 33258 (blue). Scale bar
821 indicates 30 μm (*left panels*). The ratio of fluorescent signals was normalized to nuclear

signals (*right panels*). (**B**) mRNA expression of mitochondria biogenesis-associated genes in ASCs after induction of adipocyte differentiation with or without TB in the presence of Rosi. (**C**) Western blotting of autophagy-associated proteins in ASCs after induction of adipocyte differentiation in the indicated concentration of TB in the presence of Rosi (*left panels*). The ratio of LC3-II and other proteins was normalized to LC3-I and GAPDH, respectively (*middle and right panels*). (**D**) Gene expression of LC3 (*Map1lc3a*), ATG3 (*Atg3*) and p62 (*Sqstm1*) in ASCs after induction of adipocyte differentiation with or without TB in the presence of Rosi. (**E**) Immunofluorescence analysis of LC3 (Green) in ASCs incubated with or without TB in the presence of Rosi. Nuclei were stained with Hoechst 33258 (Blue). The arrow shows the LC3-II puncta structure. Scale bar indicates 50 μm (*left panels*). The ratio of fluorescent signals was normalized to nuclear signals (*right panels*). (**B**–**D**) Data are representative of triplicate independent experiments presented as the mean ± SD (n = 3). (**B**,**D**) *$p < 0.05$; with TB vs. without TB; (**C**) Statistically significant differences between the groups are indicated by different letters ($p < 0.05$).

838 **Table 1. Browning-associated genes encoding TB-upregulated genes in subcutaneous**

839 **adipose tissue**

Gene Accession	Gene Symbol	Fold change	Category
NM_009463	*Ucp1*	183.15	brown adipocyte marker
NM_007703	*Elovl3*	29.97	beige adipocyte marker
NM_010174	*Fabp3*	9.50	brown fat cell differentiation
NM_009944	*Cox7a1*	7.18	beige adipocyte marker
NM_007702	*Cidea*	6.04	beige adipocyte marker
NM_009948	*Cpt1b*	5.54	beige adipocyte marker
NM_007751	*Cox8b*	5.03	beige adipocyte marker
NM_133904	*Acacb*	3.91	beige adipocyte marker
NM_001164047	*Mb*	3.90	brown fat cell differentiation
NM_011068	*Pex11a*	3.88	brown fat cell differentiation
NM_001163010	*Mup1*	3.27	brown fat cell differentiation
NM_010050	*Dio2*	2.35	beige adipocyte marker
NM_024437	*Nudt7*	2.28	brown fat cell differentiation
NM_009204	*Slc2a4*	2.28	brown fat cell differentiation
NM_018825	*Sh2b2*	2.13	brown fat cell differentiation
NM_029844	*Mrap*	2.03	brown fat cell differentiation
NM_009941	*Cox4i1*	2.02	beige adipocyte marker

840

841

Figure 1

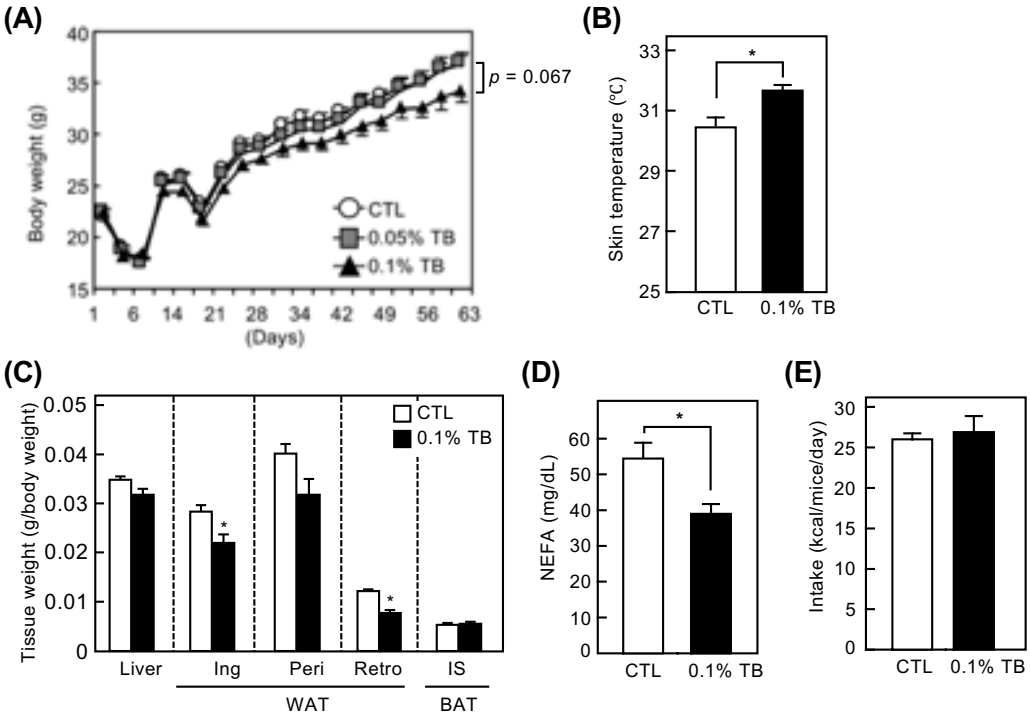

Figure 2

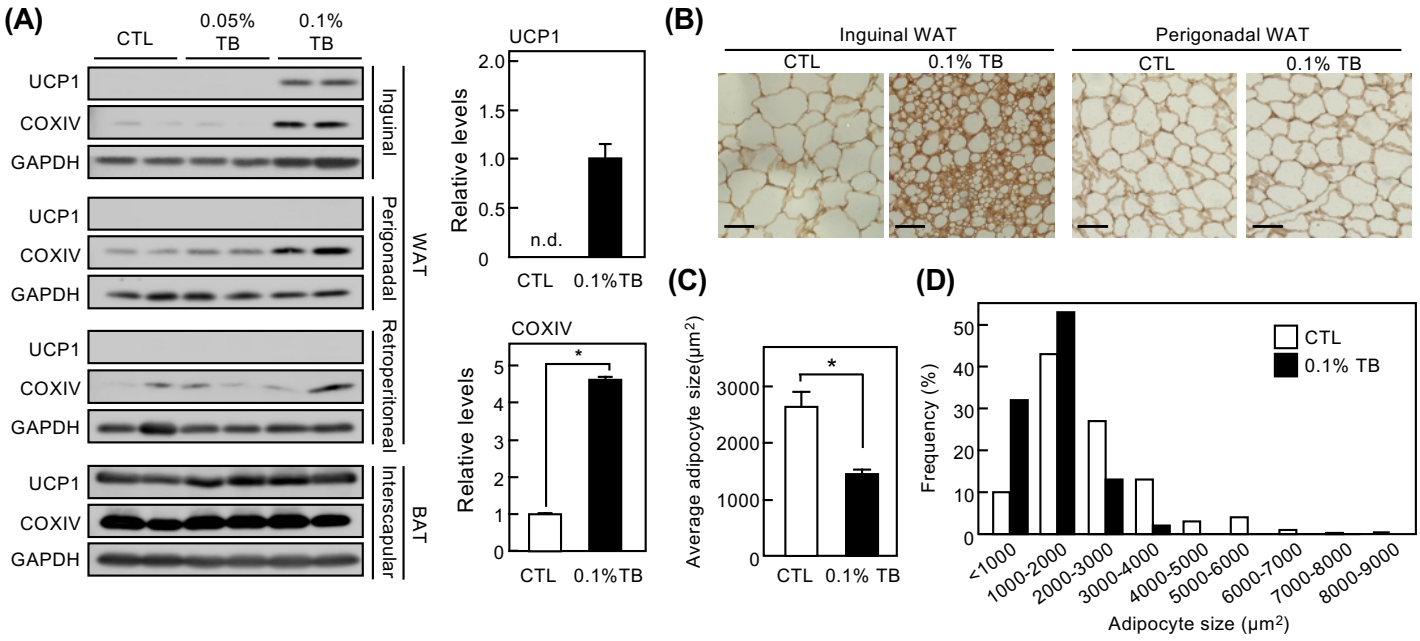

Figure 3

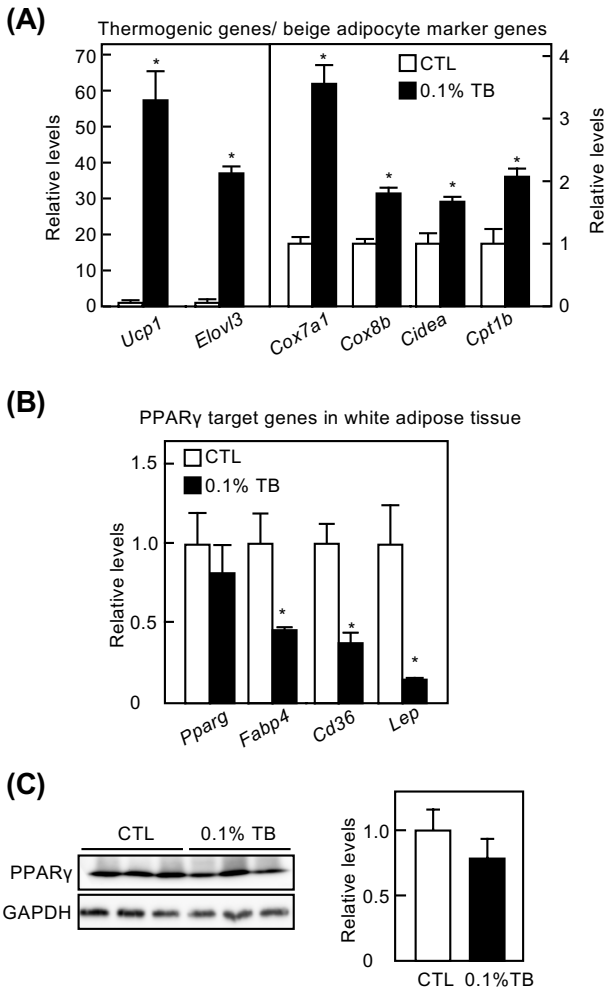

Figure 4

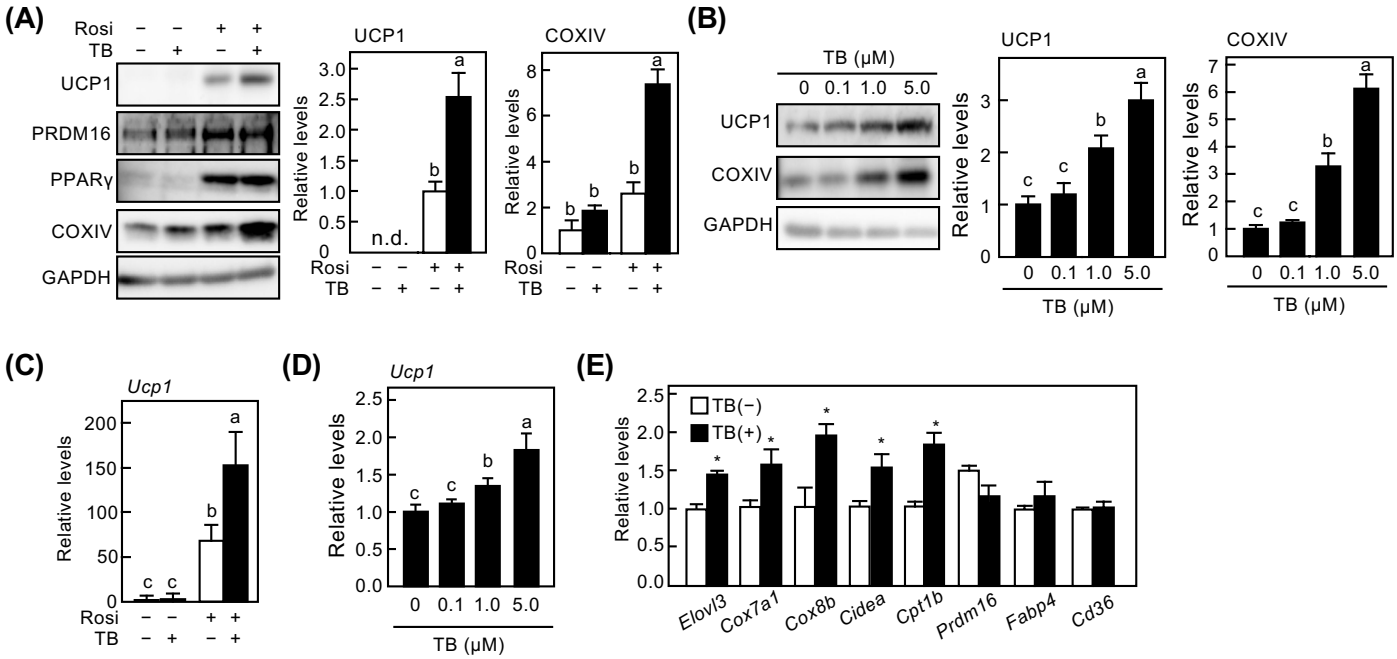

Figure 5

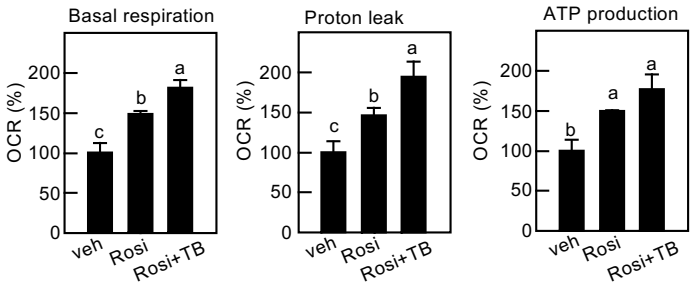

Figure 6

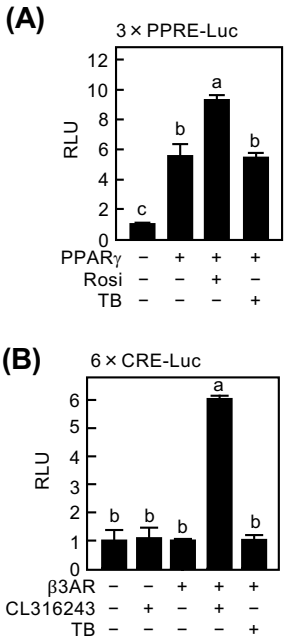

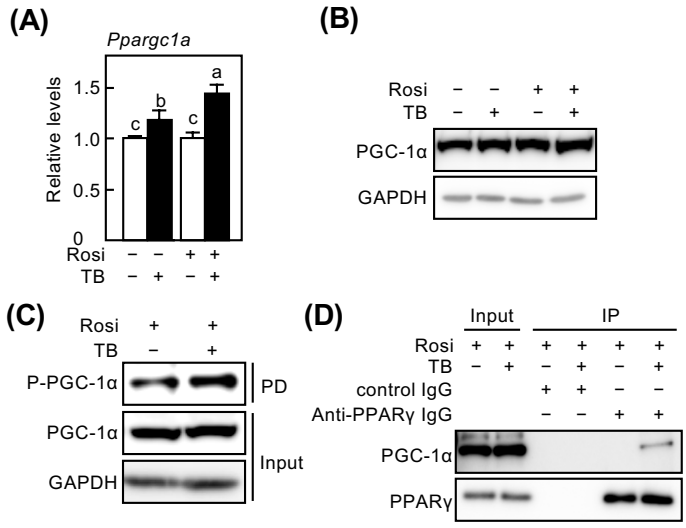

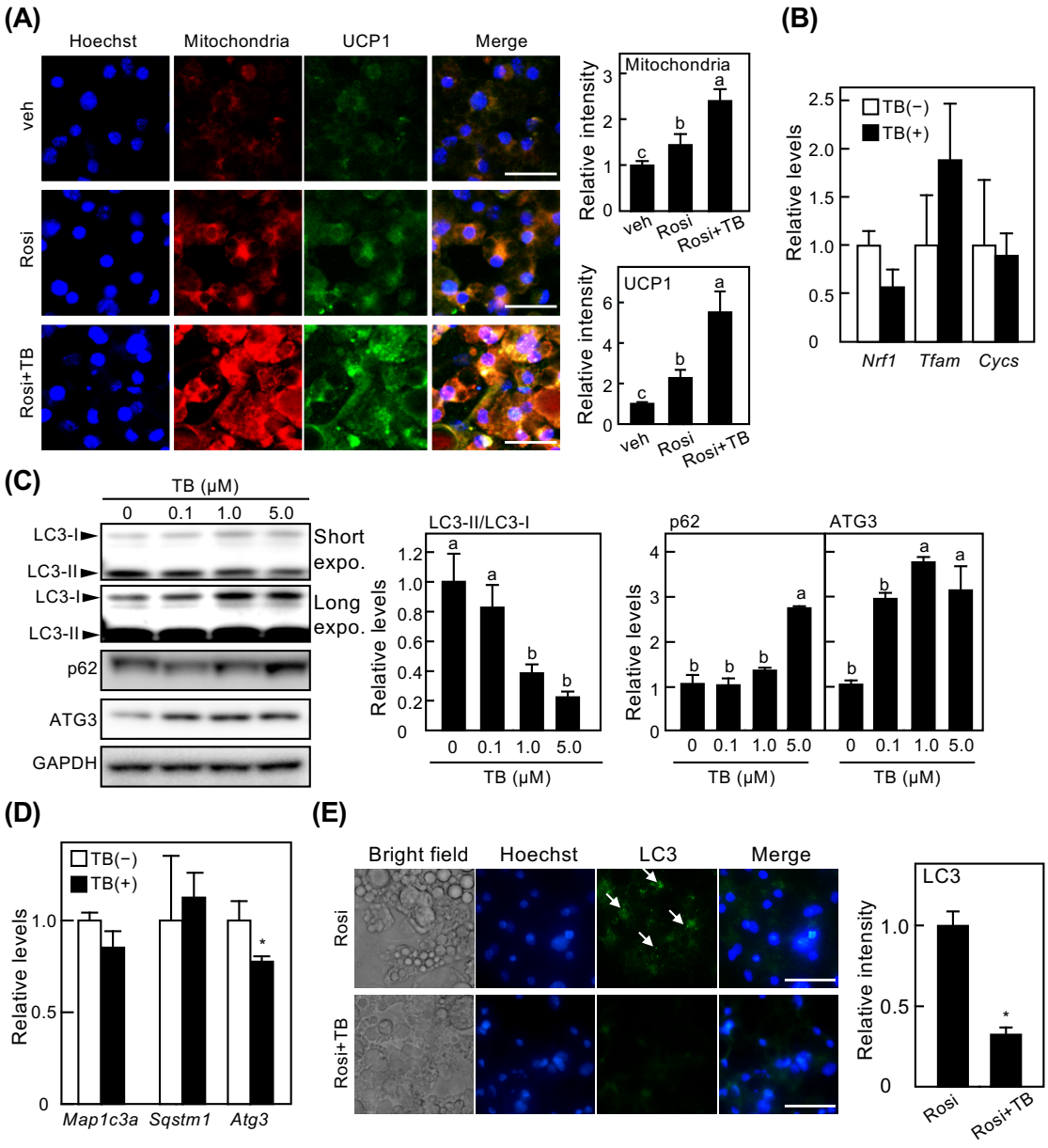

Author Statement

Emi Tanaka: Conceptualization, Methodology, Investigation, Formal analysis, Writing - Review & Editing. Takakazu Mitani: Conceptualization, Methodology, Writing - Original Draft, Writing - Review & Editing. Momona Nakashima: Investigation, Formal analysis. Eito Yonemoto: Investigation, Formal analysis. Fujii Hiroshi: Resources, Investigation, Formal analysis. Hitoshi Ashida: Formal analysis.